Adsorption and Decomposition of CWA Simulants on Single Crystal and Nanostructured Metal Oxides *(W911NF-04-1-0195)*

Dr. John R. Morris, Virginia Tech

Final Report

I. Foreword

Our studies are directed at determining the adsorption mechanisms and reaction pathways for the chemical warfare agent simulant (CWA) for GB (Sarin) on metal oxide surfaces and nanoparticles. By learning about how surface structure, nanoparticle size, composition, and surface co-adsorbates affect the overall interfacial chemistry, we are providing insight that can be applied toward the development of effective sorbent materials for protection and decontamination. Our approach couples ultrahigh vacuum (UHV) surface analysis instrumentation with precision simulant dosing capabilities to explore agent reactivity on highly characterized and contaminant-free metal oxide surfaces. Our work during this funding period has focused on studying the uptake and decomposition of the simulant dimethyl methylphosphonate (DMMP) when it impinges on the surface of nanoparticulate systems.

Table of Contents

Report Documentation Page

Form Approved
OMB No. 0704-0188

1. REPORT DATE	2. REPORT TYPE	3. DATES COVERED
2009		**00-00-2009 to 00-00-2009**

4. TITLE AND SUBTITLE	5a. CONTRACT NUMBER
Adsorption and Decomposition of CWA Simulants on Single Crystal and Nanostructured Metal Oxides	**W911NF-04-1-0195**
	5b. GRANT NUMBER
	5c. PROGRAM ELEMENT NUMBER
6. AUTHOR(S)	5d. PROJECT NUMBER
	5e. TASK NUMBER
	5f. WORK UNIT NUMBER
7. PERFORMING ORGANIZATION NAME(S) AND ADDRESS(ES)	8. PERFORMING ORGANIZATION REPORT NUMBER
Virginia Polytechnic Institute & State University,Blacksburg,VA,24060	**; 46210-CH.1**
9. SPONSORING/MONITORING AGENCY NAME(S) AND ADDRESS(ES)	10. SPONSOR/MONITOR'S ACRONYM(S)
U.S. Army Research Office, P.O. Box 12211, Research Triangle Park, NC, 27709-2211	11. SPONSOR/MONITOR'S REPORT NUMBER(S) **46210-CH.1**

12. DISTRIBUTION/AVAILABILITY STATEMENT
Approved for public release; distribution unlimited

13. SUPPLEMENTARY NOTES

14. ABSTRACT

15. SUBJECT TERMS

16. SECURITY CLASSIFICATION OF:			17. LIMITATION OF ABSTRACT	18. NUMBER OF PAGES	19a. NAME OF RESPONSIBLE PERSON
a. REPORT	b. ABSTRACT	c. THIS PAGE			
unclassified	**unclassified**	**unclassified**	**Same as Report (SAR)**	**15**	

II. Statement of the problem studied

The primary challenge in developing materials for applications, such as protective coatings and decontamination, involves first developing a detailed understanding of the surface chemistry and then applying the understanding to build specific chemical structures tailored to achieve the desired outcome. While the past decade has witnessed several key advanced in fundamental research into the uptake and decomposition of CWA simulants on a variety of metal-oxide materials, there remains surprisingly little progress toward the implementation of a practical application of nanoparticulate technology into decontamination or protection strategies. Our research aims to begin to bridge the gap between fundamental science and practical application by performing important studies on the chemistry of CWA simulants when they react on the surfaces of metal-oxide particles created under highly controlled conditions. By systematically learning the relative importance of surface structure, adsorbate concentration, and environmental conditions on particle surface chemistry, we aim to provide rules for predicting the outcome of these interactions.

III. Summary of the most important results

Experimental Development. Much of our efforts during the initial stages of this funding period were focused on developing the experimental set-up and approach for addressing our research objectives. We now operate a state-of-the-art surface science instrument and atomic force microscope in our lab dedicated to exploring the reactions of CWA simulants on a variety of surfaces. The instrumentation, described in the following paragraph, is the first of its kind designed for mechanistic studies of reactions on nanoparticle surfaces. In addition, it also serves as a surface analysis instrument for other ARO-supported research. The instrument is expected to continue to contribute to the advancement of science in general and the understanding of CWA surface chemistry far into the future.

A schematic diagram of the experimental apparatus is show below. Briefly, the experiments are performed in coupled nanoparticle synthesis and surface analysis chambers. The high-vacuum (10^{-7} Torr) synthesis chamber allows various types of metal oxide nanoparticles to be deposited on gold-coated substrates for subsequent experiments. As described further below, particle size is reproducibly varied by controlling the ambient gas pressure (0.5 to 100 Torr) to yield particles as small as 1 nm. The relative number of oxygen defects in the particles can be regulated by using oxygen or nitrogen as the ambient

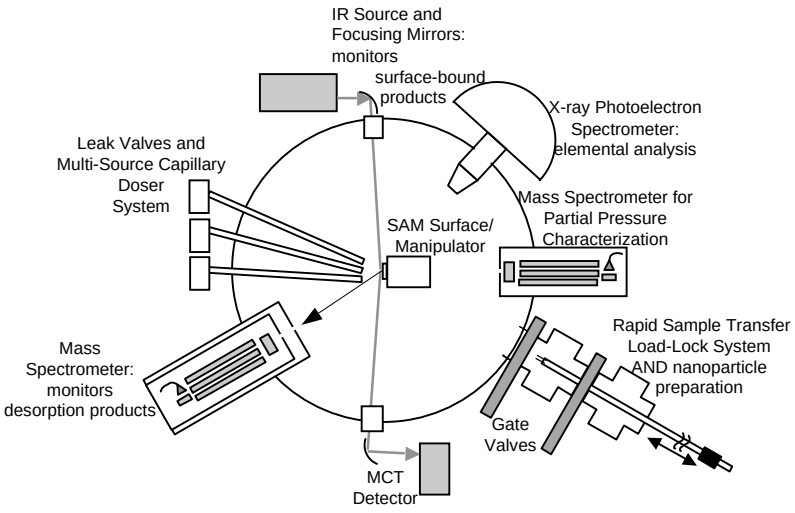

Figure 1. CWA Dosing, nanoparticle preparation, and surface analysis apparatus for investigating simulant-surface chemistry.

gas. A custom-designed sample transfer mechanism allows clean nanoparticle samples to be transferred directly into the ultrahigh-vacuum analysis chamber without exposure to air or other potential contaminants.

The ultrahigh-vacuum analysis chamber (10^{-10} Torr) ensures that: (1) neither contaminant background gases nor unwanted solvent effects contribute to the surface chemistry under investigation, (2) the surfaces remain clean and well-characterized throughout an experiment, and (3) several surface-sensitive analytical techniques can be implemented. The samples are mounted on a precision manipulator for temperature control and positioning. A load-lock system allows efficient sample introduction without venting. A leak valve equipped with a bubbler allows us to controllably dose the sample with desired simulants or other gases. During exposure to simulants, products that form on the surface are monitored with reflection-absorption infrared spectroscopy and X-ray photoelectron spectroscopy affords elemental identification of surface species.

Nanoparticle Screening for Reactivity. Using our approach of laser vaporization-nanoparticle synthesis, we have created a series of metal oxide films and nanoparticles. The primary advantage of this technique over many other approaches for nanoparticle synthesis is that it affords control over particle size in an environment where the co-adsorption of background contaminates such as water and hydrocarbons is eliminated. Isolating the particles from ambient air affords fundamental studies into the role of water and hydrocarbon contamination on uptake and reactivity, a component of our future work. With this technique, we have synthesized a series of eight different metal oxide nanoparticles in the size range of 10-50 nm as determined by transmission electron micrograph (TEM) images. The particles were vapor deposited directly onto gold-coated glass substrates to provide a reflective surface for performing reflection-absorption infrared spectroscopy (RAIRS) to probe simulant adsorption. For these initial studies, we have explored the uptake of the nerve agent simulant dimethyl methylphosphonate (DMMP), the chlorine-containing molecule 3-chlorophenol (3-CP), and the mustard simulant dibutyl sulfide (DBS). Reflection-absorption infrared spectra were recorded prior to and subsequent to gas exposure and the difference spectra are shown in Fig. 2.

To our knowledge, these experiments represent the first studies into the reactivity of Y_2O_3, HfO_2, and GdO_3 nanoparticles with DMMP and DBS. For the organophosphonate, these experiments verify previous results showing that DMMP adsorbs primarily through non-dissociative molecular interactions, likely involving P=O---M and CH_3-O(-P)---M bonding on many of the metal oxide particles. However, results for HfO_2 and ZrO_2 particles show strong evidence for dissociative adsorption with a M--O-CH_3 symmetric stretch peak at 2808 cm^{-1} (only a small peak on the scale of Fig. 2) and a significant shift and broadening of the P=O peak at ~1240 cm^{-1}. These results are significant as they identify at least two nanoparticle systems for which dissociation of the simulant DMMP occurs at room temperature. The 3-chlorophenol exposure studies (spectra not shown) indicate that this molecule sticks well to each material studied, but adsorption is largely molecular in nature with little evidence for dissociation. In contrast, the chemistry is significantly different for the uptake of the dibutyl sulfide. This molecule exhibits different degrees of reactivity on every material studied. Evidence for large quantities of surface-bound products suggests that these materials may be highly effective catalysts for the decomposition of sulfur-containing agents such as VX and HD.

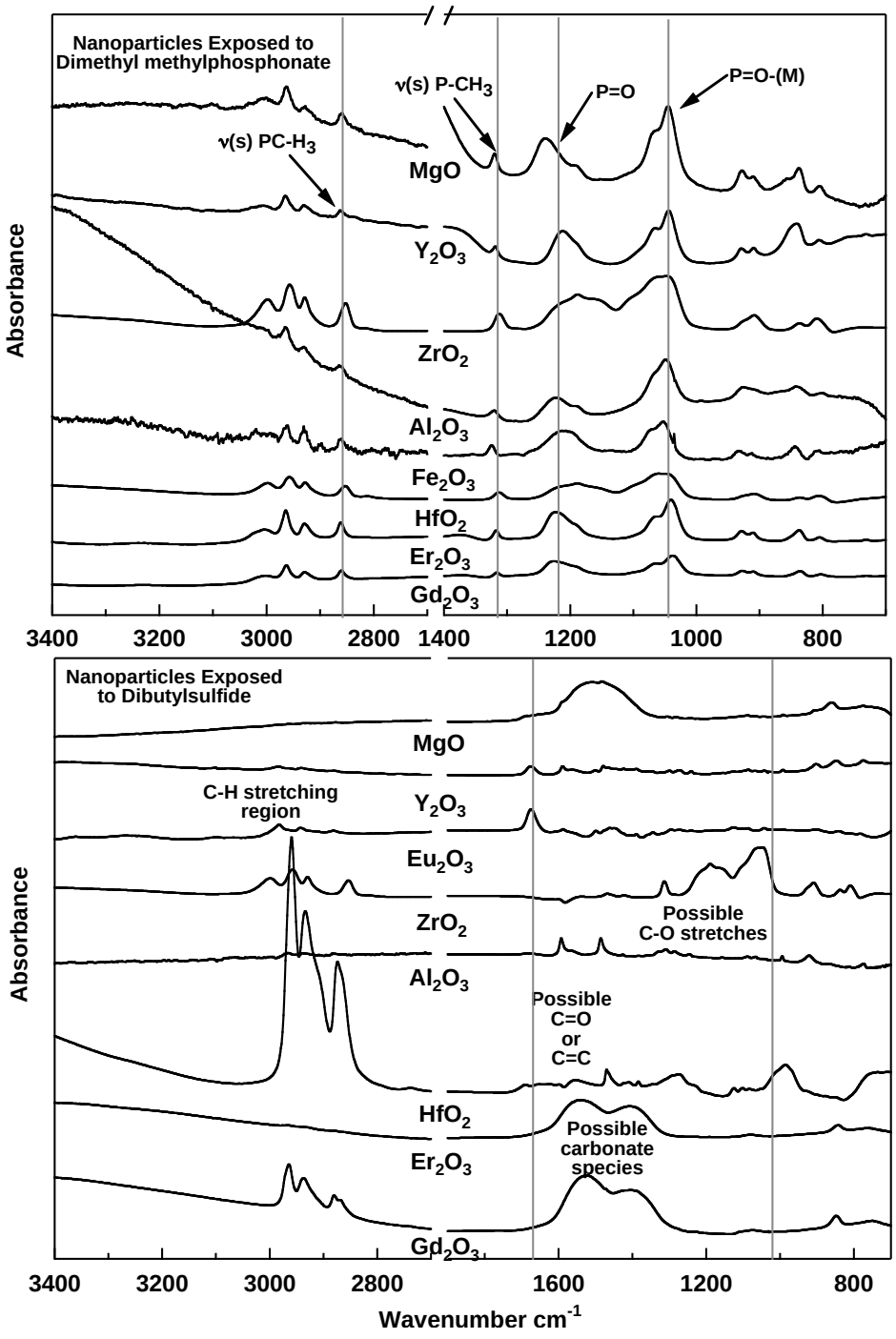

Figure 2. RAIR difference spectra for DMMP (top) and DBS (bottom) exposed to a series of nanoparticles created by laser evaporation. The nanoparticles were vapor deposited on gold substrates to facilitate the reflection-absorption infrared measurements. Only the high-energy and low-energy regions of the spectra are shown in order to highlight the important peaks. The DMMP assignments come primarily from the literature. The RAIR spectra for the DBS exposure are still unassigned and further studies are need to help elucidate the chemical nature of the surface-bound products. Note: each spectrum has been scaled to facilitate plotting them all on a single graph.

Adsorption and Decomposition of DMMP on Y_2O_3 Nanoparticles. Following extensive screening studies, as highlighted above, we identified Y_2O_3 and HfO_2 nanoparticles as promising candidates for use as sorbent materials. Specifically, our preliminary results revealed that significant DMMP decomposition and uptake occurred on these nanoparticles even after the particles were left in the ambient laboratory environment for extended periods of time. This result provided much of the motivation for further detailed studies into the fundamental mechanism of uptake and reaction of DMMP on Y_2O_3 and HfO_2 particles. The following review describes our major research accomplishments associated with studies on Y_2O_3.

Some of our most exciting results stemming from this grant have been directed toward determining the uptake probabilities and reaction pathways for DMMP and how the reactivity depends on nanoparticle size. We have recently published one of the first direct studies of particle-size effects on reactivity.

The images shown in Figure 3 are high-resolution transmission-electron micrographs of two different size Y_2O_3 nanoparticles synthesized in our lab via laser ablation techniques. The mean diameter of the particles in the upper panels are 5.8 nm and the particles in the lower panels are 2.2 nm. Also highlighted by the intersection of lines in the figure, are examples of edge and corner defect sites that are thought to be responsible for the enhanced reactivity of nanoparticles, relative to analogous planar surfaces.

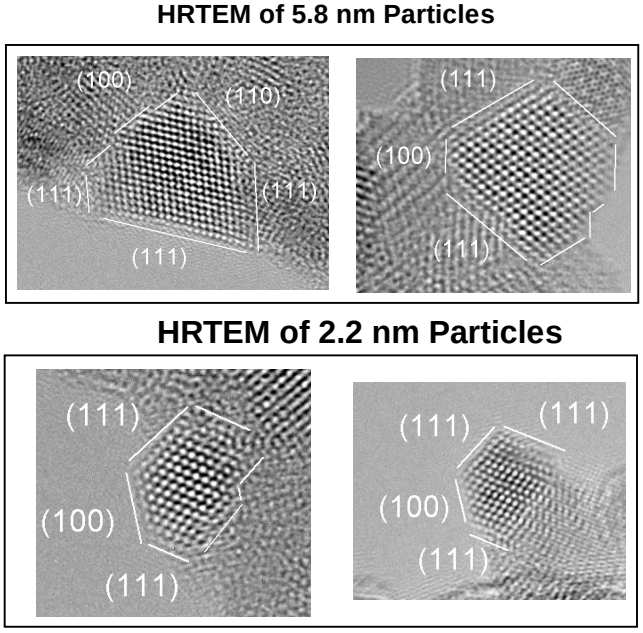

Figure 3. High-resolution TEM images of Y_2O_3 nanoparticles synthesized under different laser-evaporation conditions for control over particle size and morphology.

Using samples of the Y_2O_3 nanoparticles imaged above, we have conducted studies to determine the reaction pathways and kinetics for DMMP. Figure 4 shows *in situ* infrared spectroscopic measurements of the surface of the nanoparticles recorded during DMMP exposure. The time-resolved spectra in the upper panel reveal two key aspects of the DMMP surface chemistry: (1) the uptake probability of these molecules is high, > 70% of the molecules that interact with the particles remain on the the material at room temperature and (2) significant decomposition occurs at room temperature. The peaks labeled in black have been assigned to physisorbed DMMP and the peaks labeled in red are due to a surface-bound decomposition products that form a bridging O-P-O species. For the 5.8 nm particles, the amount of surface-bound molecular versus dissociated DMMP is approximately equal. Isotopic labeling experiments have been used to determine that the reaction mechanism procedes according to the adjacent scheme showing electrophilic attack on DMMP at a Lewis acid site.

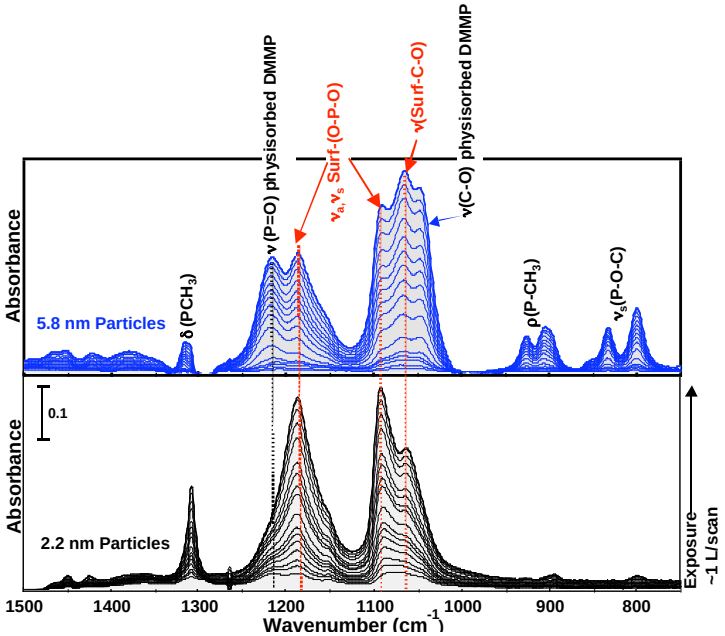

Figure 4. Infrared Spectra of DMMP uptake on the two Y_2O_3 nanoparticle samples shown in Figure 3.

The infrared data shown in the lower panel of Fig. 4 was recorded for DMMP exposed to the yttria sample composed of 2.2 nm particles. Many of the features overlap with the spectra for the larger particles, however, the signal due to physisorbed DMMP is greatly reduced. We find that the surface chemistry on the smaller particles is dominated by dissociation of surface bound products. Geometric arguments illustrate that the relative number of ions in low coordination (edge and corner) sites increases significantly with diminishing size for similarly shaped crystals. The smaller Y_2O_3 particles are inherently more reactive due to a greater percentage of atoms occupying higher energy sites. It appears that these sites near corners and edges play the most important role in the reactive uptake of simulants on nanoparticulate Y_2O_3. These results are helping to guide new studies aimed at building the most effective systems for chemical warfare agent uptake and decomposition.

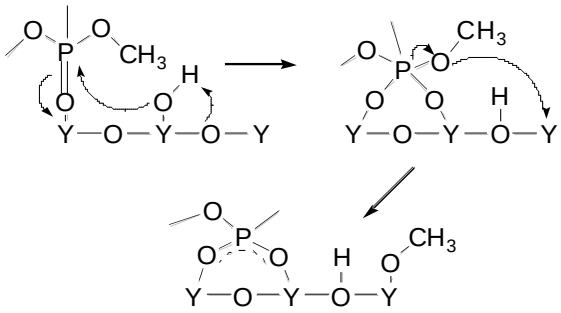

Extending initial studies. Following extensive particle screening studies and experiments into the size-effects of DMMP uptake and decomposition, we turned our experimental studies to a key system that has shown tremendous promise to serve as an active catalyst for the decomposition of agents on surfaces: TiO_2. While a great deal of research as been conducted on the photocatalytic activity of titania, little research (up to the point where we began exploring this system) has been conducted into the chemistry

of simulants, in particular DMMP, on titania particles in the dark and under the well-controlled conditions afforded by our ultrahigh vacuum approach. Our research into the chemistry of DMMP on titania has lead to numerous new discoveries that are described in detail in the papers published throughout the duration of this grant. Some of the key accomplishments are:

1. We have synthesized and characterized, with atomic force microscopy (AFM), XPS, and RAIRS, an array of different size TiO_2 particles in the range of 5-20 nm. This accomplishment is significant because it represents the first time that titania particles have been synthesized in vacuum in our lab where they are free from the atmospheric contaminants and reagents that are always present when using other preparation techniques.

2. We have extensively studied the decomposition pathways of DMMP and methanol on Degusa P-25 nanoparticles. These studies have revealed the mechanism for initial uptake and decomposition. Furthermore, we have found that extended exposure or thermal cycling of TiO_2 leads to the formation of a passivating Ti-O-P-O-Ti layer that insulates the active sites against further reactivity.

3. We have developed a new transmission FTIR approach for exploring electronic excitations that occur within semiconductor nanoparticles, such as titania. This approach enables us to track simultaneously the vibrational structure of molecules adsorbed onto the particles and the nature of trapped surface electrons that are easily generated on reduced titania.

Experimental details. Overall, our results into DMMP chemistry on titania have, not only reproduced previous work in this area, but we have also advanced the fundamental understanding of the decomposition mechanism by employing an FTIR technique that enables us to track conduction-band electrons during the reaction. The key to this technique involves the use of the sample holder shown in Figure 5. The holder consists of a fine (80% transmittance) tungsten mesh into which a particular nanoparticle sample is embedded. The nanoparticles are pressed into the grid in a manner that fills the voids, yet still enables infrared radiation to pass through; thereby, enabling traditional transmission infrared studies to be performed on metal-oxide nanoparticles. The grid can be resistively heated to 800 K and readily cooled to liquid nitrogen temperatures. This added capability to our research has enabled us to track several new aspects of the surface chemistry of nanoparticulate materials.

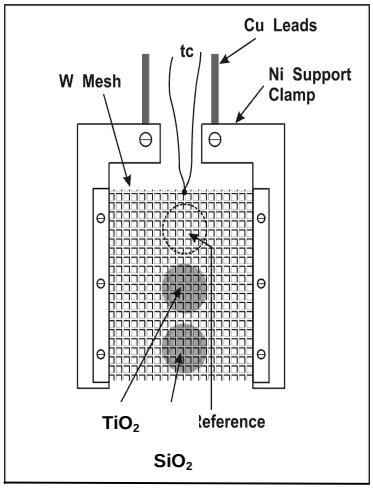

Figure 5. Nanoparticle sample holder for transmission FTIR studies.

Reaction pathways on TiO_2. The majority of our experiments during the latter portion of our funding cycle have employed the sample holder described above to study the decomposition of DMMP on titania of varying particle sizes. Figure 6 shows the

FTIR data for surface-adsorbed DMMP during exposure. We find that the initial uptake of DMMP on clean, fully oxidized titania is every efficient. The spectrum shown following 1 minute of exposure at 0.8 Torr of DMMP reveals that the molecules interact initially with surface hydroxyl groups and readily decompose to form a surface-bound carbonyl, as evidenced by the strong peak at 1700 cm^{-1}. However, this product appears to decompose very efficiently on the surface into carbonates that remain strongly bound to the titania throughout the experiment. One of the key peaks in this spectrum is the mode assigned to an O-P-O stretch at ~1075 cm^{-1}. We find that this species is responsible for the poisoning of active surface sites and cannot be removed even after extensive thermal cycling. In fact, the adsorption of DMMP changes from predominately dissociative to molecular after just two cycles of dosing and heating to 700 K.

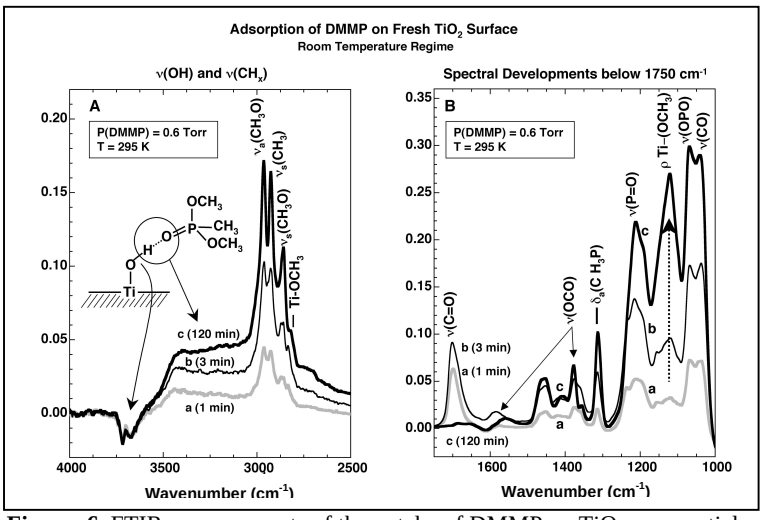

Figure 6. FTIR measurements of the uptake of DMMP on TiO_2 nanoparticles.

Direct involvement of lattice oxygen in TiO_2 surface chemistry. The above studies revealed a great deal of information about the room-temperature reactions of DMMP of titania and provided the foundation for investigations into the role of conduction band electrons in decomposing adsorbates at elevated temperatures. The FTIR data shown in Figure 7 reveals how the absorbance changes as the titania surface sample is exposed to DMMP and systematically heated to 675 K. As the temperature is raised, we observe two key changes in the spectra: *(i)* the overall absorbance, over the entire mid-infrared range, increases dramatically, and *(ii)* the peaks

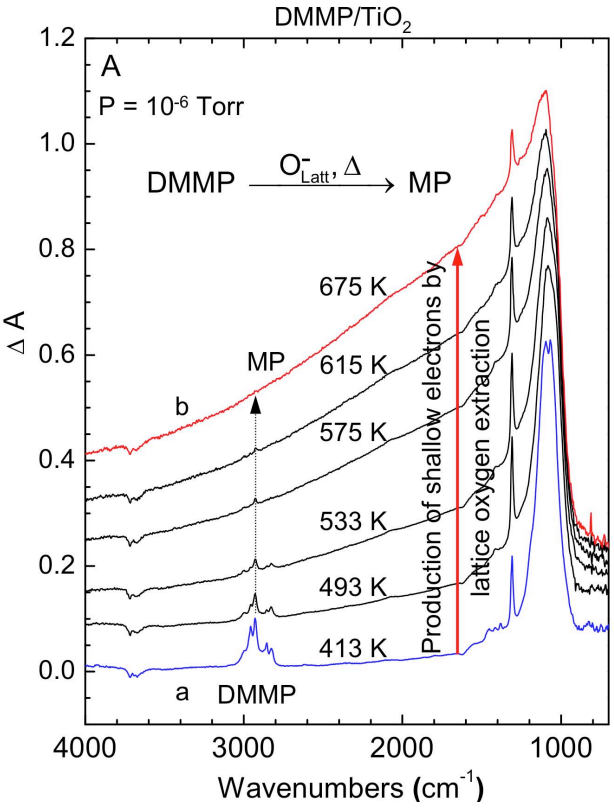

Figure 7. Infrared spectra of DMMP on TiO_2 particles during one heating cycle to 675K. The overall rise is due to the production of conduction band electrons trapped within the particles or at the surface.

associated with adsorbed DMMP and its decomposition products diminish. We have performed a series of similar experiments using methanol and alternate surface preparation techniques to learn that these effects are the result of the extraction of lattice oxygen from the TiO_2 during heating. Specifically, we now understand that the broad background absorbance observed upon heating is due to the production of conduction-band electrons that occurs when lattice oxygen is removed from titania upon reduction of the material. For a clean TiO_2 sample, the oxygen ions simply recombine on the surface or react to desorb as O_2; however, the DMMP adsorbate appears react efficiently with the labile oxygen. The primary decomposition product is surface-bound methyl phosphate (MP) and a bridging Ti-O-P-O-Ti layer, as evidenced by the development of a single peak around 3000 cm^{-1} and broad feature at 1000 cm^{-1}, respectively. These experiments have shown, for the first time, that there is a direct linear relationship between the production of conduction band electrons (removal of lattice oxygen) and the decomposition of the adsorbed DMMP at elevated temperatures.

Thermal cycling and poisoning of TiO_2. Further experiments have probed the thermal cycling of DMMP-exposed TiO_2 to assess the potential of regenerating active surface sites for the continued decomposition of agents. Figure 8 shows three heating cycles similar to the temperature ramp in Figure 7. The peak in the absorbance that is highlighted with an arrow represents a carbonyl stretch that emerges and the primary dissociation product upon adsorption on clean nanoparticulate titania. This peak is significantly reduced upon the second exposure and nearly completely absent by just the third exposure and heating cycle. Furthermore, the relative amount of physisorbed DMMP increases markedly across the three exposure cycles and the IR intensity diminishes significantly in the region from 1200 cm^{-1} to 900 cm^{-1}, as highlighted by the circled region of the spectra. The missing bands in this low-wavenumber region is due to complete absorbance of the IR radiation by the sample across this entire range. The nearly negligible transmittance results from the formation of a Ti-O-P-O-Ti network that effectively coats the particles during repeated heating and exposure. It appears that this network is also responsible for shielding the active surface sites from incoming DMMP.

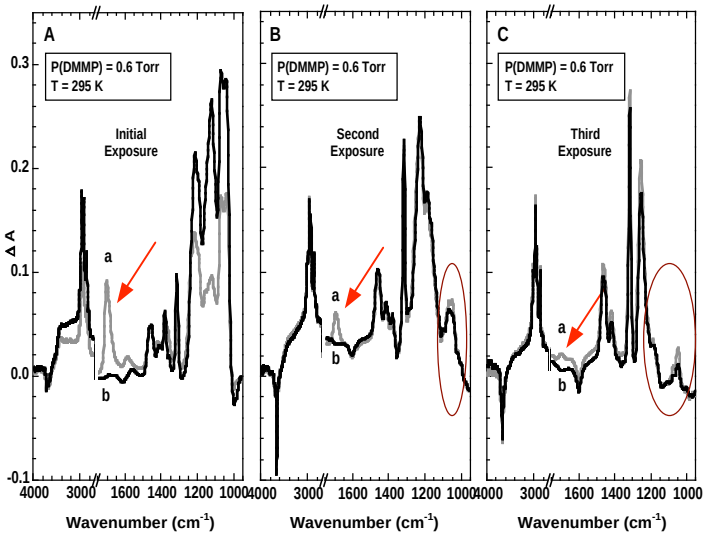

Figure 8. Thermal cycling of TiO_2 exposed to DMMP.

Our experiments during on pure titania have revealed that clean 25 nm TiO_2 particles are highly active toward the uptake and decomposition of the simulant DMMP. The initial binding to the surface is through the formation of a hydrogen bond between the phosphoryl group of the DMMP and surface hydroxyl species. Following initial binding, the DMMP appears to diffuse or begin to adsorb to more reactive sites where

decomposition leads to carboxylic acid formation, a methoxy species, and organic phosphates. However, the ultimate fate of these surface adsorbates appears to be complete decomposition to a phosphorous-titania network that covers the particles and insulates them from further reactions with DMMP. The decomposition is aided by lattice oxygen, liberated from the particles at elevated temperatures, which attacks the adsorbates, as illustrated in Figure 9. Our next stage in this research built on these findings by focusing on mixed metal-titania nanomaterials in an effort to identify systems for which reactivity is truly catalytic.

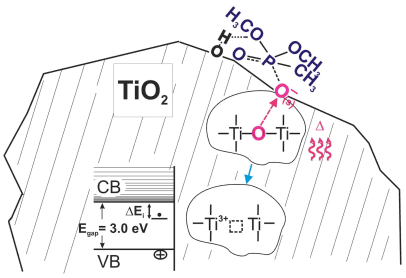

Figure 9. Schematic depiction of the chemistry responsible for the decomposition of adsorbed DMMP at elevated temperatures. The figure shows the generation of trapped electrons as oxygen is released from the bulk of the particles during thermal reduction of the material. The trapped electrons are probed by FTIR because they lie very close in energy to the conduction band continuum into which they are promoted upon IR absorption.

Catalytic oxidation of DMMP on TiO_2-supported Au nanoparticles. Following our studies into the role of lattice oxygen in TiO_2 surface chemistry, we focused on exploring the possibility of rendering TiO_2 catalytic by incorporating Au atoms, nanoparticles, or thin films into the titania support. Other groups have observed increased catalytic activity of Au-coated particles for the decomposition of CO_2 and other organic gases. Our studies are the first to demonstrate that CWA simulants also decompose on the mixed nanoparticulate materials. We hypothesize that the nano-scale gold particles are reactive enough to activate the titania, yet inert toward the formation of a passivating phosphate layer. Results on this system highlight the promise of the approach to create active catalysts that are resistant to poisoning by phosphate adsorption.

We have used infrared spectroscopy to investigate the uptake and decomposition of dimethyl methylphosphonate on TiO_2-supported Au nanoparticles. The experiments were performed by mounting a pure TiO_2 sample adjacent to the Au-TiO_2 sample to compare the relative reactivity of the two materials simultaneously. Since the samples were mounted on the same support, they experienced identical exposure durations and experimental conditions. Comparisons were made by simply alternating samples into and out of the path of the infrared radiation.

Figure 10 shows a direct comparison of the uptake of DMMP on the pure TiO_2 and the Au-TiO_2 samples. The spectra were recorded under vacuum following exposure of the samples to 20 Torr of DMMP for two minutes. The Au-TiO_2 (blue) and pure-TiO_2 (red) spectra agree closely in the region of the CH-stretch vibrations (above 2500 cm^{-1}) and in the region of CH-deformation modes, P=O, and methoxy C-O stretching vibrations (below 1500 cm^{-1}), suggesting a similar mechanism of DMMP uptake on the surfaces of both samples. Molecular physisorption of DMMP on the open TiO_2 regions of each sample occurs readily at 295 K. In addition, partial decomposition of DMMP occurs on the titania regions of both samples through reactions involving traces of active oxygen. The primary products of the hydrolysis are methanol and/or surface methoxy species, as revealed by the small band at 2819 cm^{-1} in both spectra.

Although the high and low energy spectral regions of Fig. 10 are nearly identical, the mid-region exhibits several key differences that are attributed to oxidation on the Au-TiO_2 surface. Strong bands are observed due to surface-bound aldehyde (~ 1740-1720 cm^{-1}) and carboxylic acid (~ 1680-1650 cm^{-1})[1] products. The broad band at ~ 1560 cm^{-1} suggests the formation of formate or carboxylate on Au-TiO_2. [2-5] In addition, bands around 2100 cm^{-1} show that the Au-TiO_2 is active enough to form surface-bound carbon monoxide, a clear indication of the DMMP oxidation.[3] In contrast, no CO bands have ever been detected on pure-TiO_2 following DMMP exposure in the absence of UV

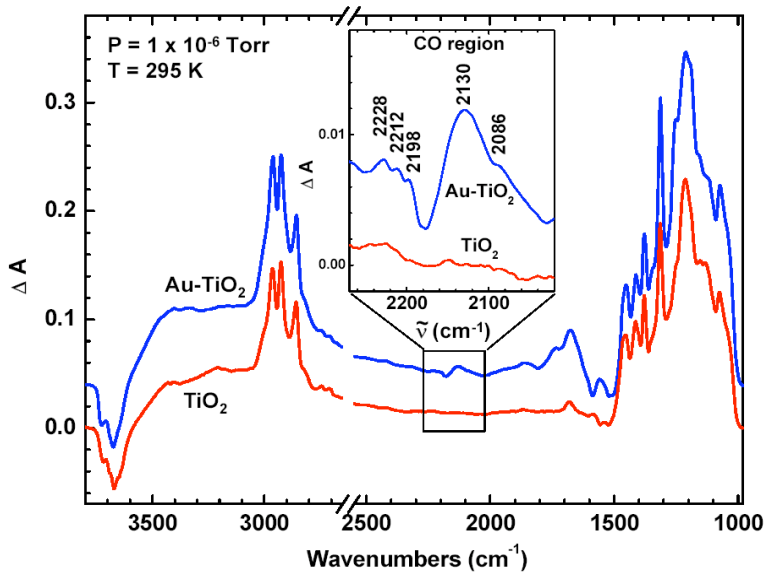

Figure 10. A comparison between the FTIR difference spectra of Au/TiO_2 and pure TiO_2 nanoparticles following 2 min exposure to DMMP. The inset highlights the CO region of the spectra.

radiation. The high reactivity of the Au-TiO_2 is likely due to a combination of factors,[6] including the presence of highly reactive surface oxygen.[7-10]

In addition to providing information about the major surface-bound products, the infrared spectra enable us to monitor the oxidation state of the Au particles during the reaction. Previous theoretical[11] and experimental[12,13] studies have shown that the vibrational frequency of surface-bound CO is highly sensitive to the site of adsorption on Au surfaces. The inset in Fig. 10 shows that CO is adsorbed on metallic Au^0 sites (ν_{CO} = 2086 cm^{-1}), on positively polarized gold $Au^{\delta+}$ sites (ν_{CO} = 2130 cm^{-1}),[10,14] and on CUS Ti^{4+} (ν_{CO} = 2198 - 2212 cm^{-1}).[2,7,8,10,14] The presence of oxidized gold and unsaturated titanium suggests that lattice oxygen is extracted during the reaction with DMMP. Since analogous oxidation products (formate and CO) are not observed on the pure TiO_2 sample, it appears that gold promotes the extraction of lattice oxygen.[10,15] However, we cannot exclude the presence of some unsaturated titanium sites on the surface of as-prepared Au-TiO_2 before the adsorption of DMMP, as reported by others.[9,10]

Oxygen activation. Once the surface oxygen is depleted under anaerobic conditions, the initial high reactivity of the Au-TiO_2 particles slows considerably. However, we find evidence for regeneration of active surface oxygen and a second reaction mechanism occurring upon the admittance of O_2 into the system. Regeneration of active surface

oxygen occurs upon introduction of a small amount of O_2 to the particles. Figure 11 shows difference spectra obtained when both pure titania and gold-titania samples were exposed to O_2(g). The IR spectrum of DMMP adsorbed on pure TiO_2 (f in Fig. 11) changes very little during oxygen exposure, even at the highest pressure of 10 Torr O_2. In stark contrast to the inactivity of the pure particles, the IR spectra show significant changes when Au is present on TiO_2. The primary product peak for the Au-TiO_2 occurs at 1550 cm^{-1}, indicative of the production of formate/carboxylate species. The many spectral changes in the region below 1500 cm^{-1} are caused by the simultaneous production of formate, carboxylate, and carbonate species, and the thermal desorption of DMMP. Other products include RC=O (1728 cm^{-1}), RCOOH (1682 cm^{-1}), and hydrocarbon species (2850, 2925 and 2972 cm^{-1}). In fact, some of the adsorbates are oxidized completely to CO_2, as evidenced by the small bands at 2360 and 2330 cm^{-1} in spectrum 'e'. The only precedence for complete oxidation of DMMP by molecular oxygen at room temperature on TiO_2 involves the use of UV radiation to produce conduction-

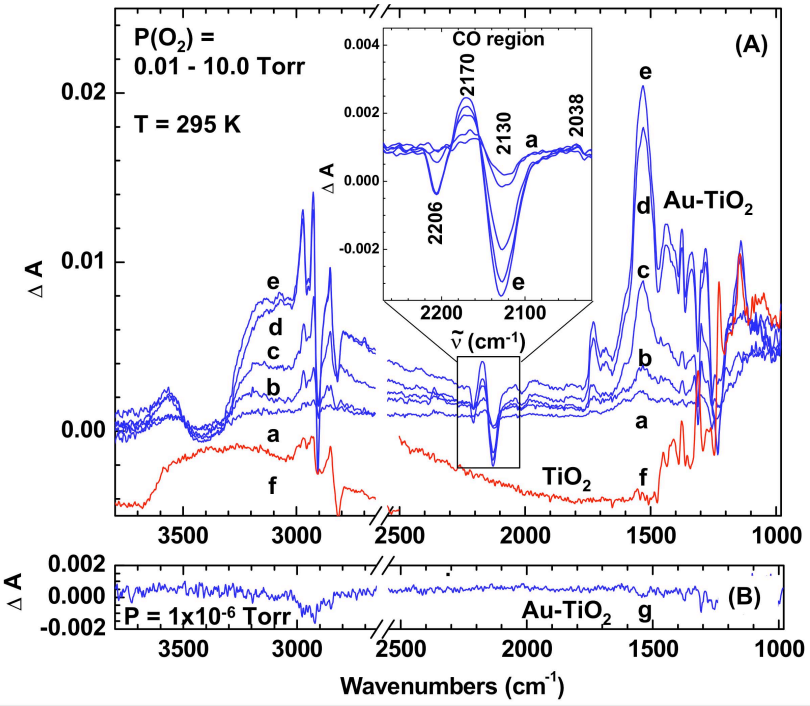

Figure 11. (A) Difference spectra for the samples shown in Fig. 10 upon exposure to O_2(g). The inset highlights the CO region of the spectra for the Au/TiO_2 sample. (B) Difference spectrum of the Au/TiO_2 sample recorded after evacuation to show that the products remain surface bound.

band electrons, which activate the oxygen.[3-5] In this study, we observe the production of similar products, but in the dark and at room temperature.

In addition to the surprising activity of the Au-TiO_2 particles at room temperature, we find the oxidative chemistry of adsorbed DMMP is further enhanced on this sample upon heating. When the samples containing adsorbed DMMP are exposed to molecular O_2 at 475 K, intense combustion of $DMMP_{(a)}$ occurs to form gas-phase CO_2 and intermediate products of partially oxidized organic species. The progression of DMMP oxidation is evident from the negative IR features of Fig. 12 (Panel A, spectra a - d) for the methoxy groups: $\nu(CH_3O)$ modes (2950 cm^{-1} and 2850 cm^{-1}) and by the positive features at ~ 2360 cm^{-1} and ~ 2337 cm^{-1} corresponding to gas-phase CO_2, a product of complete combustion.

The evolution of gas-phase CO_2 is shown more clearly by inset D of Fig. 12, which is a spectrum of the pure vapor phase during the reaction.

In contrast to the significant oxidation observed on the Au/TiO_2 sample, Fig. 12 (panel B) shows no evidence for decomposition of DMMP on the pure-TiO_2 sample, even after 45 min of oxygen exposure at 475 K. The only spectroscopic changes for this sample are the negative IR modes due to desorption of physisorbed DMMP, as previously observed.[16] Therefore, the spectral developments observed for the Au-TiO_2 are caused entirely by the presence of Au nanoparticles on this sample.

The spectral signature of the adsorbed CO provides further insight into the overall reaction mechanism by revealing details about the oxidation state of the gold to which it is bound. Our studies, which show cycling of the oxidation state of the Au particles during the decomposition of DMMP, have been used in conjunction with previous work

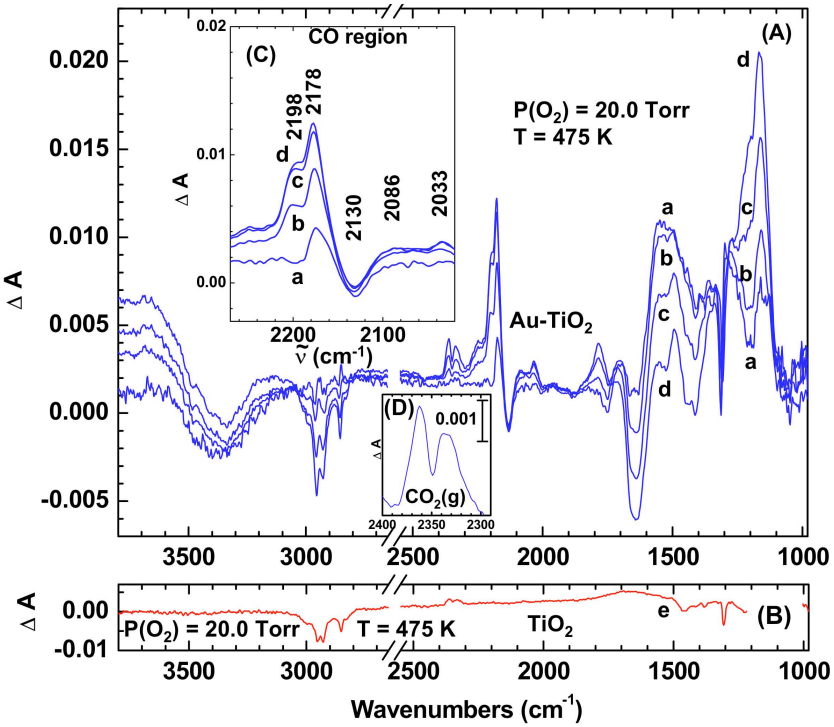

Figure 12. (A) Spectral changes for the Au/TiO_2 sample after admittance of 10 Torr O_2: a – 1 min; b – 4 min; c – 25 min; d – 50 min; e – 45 min. The inset C highlights the CO region of the spectra for the Au/TiO_2 sample and the inset D highlights the CO_2 region of the spectra for the gas phase CO_2. (B) Spectral changes for the TiO_2 sample after 45 min of oxygen exposure. The peaks at 2350 cm^{-1} in the pure TiO_2 spectrum are from the production of gas phase CO_2 created on the Au-TiO_2 sample and then filling the volume of the vacuum chamber where the pure sample also resides.

to provide a description of the overall mechanism of oxidation.[11,17-22] Details of the mechanism are discussed in detail in the publications listed in this final report. Briefly, we find that the activation of oxygen involves charge transfer from a $Au^{\delta+}$ site residing at the periphery of a Au particle to form an active oxygen species, probably O_2^-. The extremely strong oxidant, O_2^-, readily reacts with physisorbed DMMP through a chain of consecutive steps to produce organic products, P-O_x residues, and gas-phase CO and CO_2.

The results from this work suggest that TiO_2-supported Au catalysts may be an effective strategy for addressing many of the practical and technical challenges associated

with pure TiO_2 photocatalysts. Unlike traditional photocatalytic approaches for decomposing CWAs on titania, the Au-TiO_2 system does not require UV radiation and our results suggest that the Au catalyst is not poisoned in the same way as the pure TiO_2 particles. Advancing the overall understanding of the catalytic mechanism and learning how the physical characteristics of the particles affect activity for two key classes of CWA simulants forms the basis for our future work.

IV. References

(1) Chuang, C.-C.; Wu, W.-C.; Huang, M.-C.; Huang, I. C.; Lin, J.-L. *FTIR Study of Adsorption and Reactions of Methyl Formate on Powdered TiO2*; J. Catal., 1999, **185**, 423-434.

(2) Liao, L. F.; Lien, C. F.; Shieh, D. L.; Chen, M. T.; Lin, J. L. *FTIR Study of Adsorption and Photoassisted Oxygen Isotopic Exchange of Carbon Monoxide, Carbon Dioxide, Carbonate, and Formate on TiO₂*; J. Phys. Chem. B, 2002, **106**, 11240-11245.

(3) Rusu, C. N.; Yates, J. T. *Photooxidation of Dimethyl Methylphosphonate on TiO2 Powder*; J. Phys. Chem. B, 2000, **104**, 12299-12305.

(4) Moss, J. A.; Szczepankiewicz, S. H.; Park, E.; Hoffmann, M. R. *Adsorption and Photodegradation of Dimethyl Methylphosphonate Vapor at TiO₂ Surfaces*; J. Phys. Chem. B, 2005, **109**, 19779-19785.

(5) Trubitsyn, D. A.; Vorontsov, A. V. *Experimental Study of Dimethyl Methylphosphonate Decomposition over Anatase TiO₂*; J. Phys. Chem. B, 2005, **109**, 21884-21892.

(6) Janssens, T.; Clausen, B.; Hvolbæk, B.; Falsig, H.; Christensen, C.; Bligaard, T.; Nørskov, J. *Insights into the reactivity of supported Au nanoparticles: combining theory and experiments*; Top. Catal., 2007, **44**, 15-26.

(7) Boccuzzi, F.; Chiorino, A.; Tsubota, S.; Haruta, M. *FTIR Study of Carbon Monoxide Oxidation and Scrambling at Room Temperature over Gold Supported on ZnO and TiO2. 2*; J. Phys. Chem., 1996, **100**, 3625-3631.

(8) Venkov, T.; Fajerwerg, K.; Delannoy, L.; Klimev, H.; Hadjiivanov, K.; Louis, C. *Effect of the activation temperature on the state of gold supported on titania: An FT-IR spectroscopic study*; Appl. Catal. A, 2006, **301**, 106-114.

(9) Panayotov, D. A.; Yates, J. T. *Spectroscopic Detection of Hydrogen Atom Spillover from Au Nanoparticles Supported on TiO2: Use of Conduction Band Electrons*; J. Phys. Chem. C, 2007, **111**, 2959-2964.

(10) Liu, H.; Kozlov, A. I.; Kozlova, A. P.; Shido, T.; Asakura, K.; Iwasawa, Y. *Active Oxygen Species and Mechanism for Low-Temperature CO Oxidation Reaction on a TiO2-Supported Au Catalyst Prepared from Au(PPh3)(NO3) and As-Precipitated Titanium Hydroxide*; J. Catal., 1999, **185**, 252-264.

(11) Wang, J.; Hammer, B. *Oxidation state of oxide supported nanometric gold*; Top. Catal., 2007, **44**, 49-56.

(12) Chen, M. S.; Cai, Y.; Yan, Z.; Goodman, D. W. *On the Origin of the Unique Properties of Supported Au Nanoparticles*; J. Am. Chem. Soc., 2006, **128**, 6341-6346.

(13) Boccuzzi, F.; Chiorino, A.; Manzoli, M.; Lu, P.; Akita, T.; Ichikawa, S.; Haruta, M. *Au/TiO2 Nanosized Samples: A Catalytic, TEM, and FTIR Study of the Effect of Calcination Temperature on the CO Oxidation*; J. Catal., 2001, **202**, 256-267.

(14) Grunwaldt, J.-D.; Maciejewski, M.; Becker, O. S.; Fabrizioli, P.; Baiker, A. *Comparative Study of Au/TiO2 and Au/ZrO2 Catalysts for Low-Temperature CO Oxidation*; J. Catal., 1999, **186**, 458-469.

(15) Scire, S.; Minico, S.; Crisafulli, C.; Satriano, C.; Pistone, A. *Catalytic combustion of volatile organic compounds on gold/cerium oxide catalysts*; Appl. Catal. B, 2003, **40**, 43-49.
(16) Rusu, C. N.; Yates, J. T. *Adsorption and Decomposition of Dimethyl Methylphosphonate on TiO2*; J. Phys. Chem. B, 2000, **104**, 12292-12298.
(17) Wang, J. G.; Hammer, B. *Role of Au[sup +] in Supporting and Activating Au[sub 7] on TiO[sub 2](110)*; Phys. Rev. Lett., 2006, **97**, 136107.
(18) van Bokhoven, J. A.; Louis, C.; Miller, J. T.; Tromp, M.; Safonova, O. V.; Glatzel, P. *Activation of Oxygen on Gold/Alumina Catalysts: In Situ High-Energy-Resolution Fluorescence and Time-Resolved X-ray Spectroscopy*; Angew. Chem. Int. Ed., 2006, **45**, 4651-4654.
(19) Laursen, S.; Linic, S. *Oxidation Catalysis by Oxide-Supported Au Nanostructures: The Role of Supports and the Effect of External Conditions*; Phys. Rev. Lett., 2006, **97**, 026101.
(20) Guzman, J.; Gates, B. C. *Catalysis by Supported Gold: Correlation between Catalytic Activity for CO Oxidation and Oxidation States of Gold*; J. Am. Chem. Soc., 2004, **126**, 2672-2673.
(21) Fierro-Gonzalez, J.; Guzman, J.; Gates, B. *Role of cationic gold in supported CO oxidation catalysts*; Top. Catal., 2007, **44**, 103-114.
(22) Weiher, N.; Beesley, A. M.; Tsapatsaris, N.; Delannoy, L.; Louis, C.; vanBokhoven, J. A.; Schroeder, S. L. M. *Activation of Oxygen by Metallic Gold in Au/TiO2 Catalysts*; J. Am. Chem. Soc., 2007, **129**, 2240-2241.